NeuroToxicology 34 (2013) 95–104

Contents lists available at SciVerse ScienceDirect

NeuroToxicology

Ethanol modulates the neurovascular coupling

Michael Luchtmann [a,*], Katja Jachau [b,1], Daniela Adolf [c,2], Friedrich-Wilhelm Röhl [c,2], Sebastian Baecke [c,2], Ralf Lützkendorf [c,2], Charles Müller [c,2], Johannes Bernarding [c,2]

[a] Department of Neurosurgery, Otto-von-Guericke-University Magdeburg, Institute for Biometry and Medical Informatics, Otto-von-Guericke-University Magdeburg, Leipziger Str. 44, 39120 Magdeburg, Germany
[b] Institute for Forensic Medicine, Otto-von-Guericke-University Magdeburg, Leipziger Str. 44, 39120 Magdeburg, Germany
[c] Institute for Biometry and Medical Informatics, Otto-von-Guericke-University Magdeburg, Leipziger Str. 44, 39120 Magdeburg, Germany

ARTICLE INFO

Article history:
Received 6 September 2012
Accepted 29 October 2012
Available online 14 November 2012

Keywords:
Ethanol
BOLD
Neurovascular coupling
Hemodynamic response
Balloon model
Hemodynamic modeling

ABSTRACT

Despite some evidence of the underlying molecular mechanisms the neuronal basis of ethanol-induced effects on the neurovascular coupling that forms the BOLD (blood oxygenation level dependent) signal is poorly understood. In a recent fMRI (functional magnetic resonance imaging) study monitoring ethanol-induced changes of the BOLD signal a reduction of the amplitude and a prolongation of the BOLD signal were observed. However, the BOLD signal is assumed to consist of a complex superposition of different underlying signals. To gain insight how ethanol influences stimulus efficacy, oxygen extraction, transit time and vessel-related parameters the fMRI time series from the sensori-motor and the visual cortex were analyzed using the balloon model. The results show a region-dependent decrease of the stimulus efficacy to trigger a post-stimulus neurovascular response as well as a prolongation of the transit time through the venous compartment. Oxygen extraction, feedback mechanisms and other vessel-related parameters were not affected. The results may be interpreted as follows: the overall mechanisms of the neurovascular coupling are still acting well at the moderate ethanol level of about 0.8‰ (in particular the vessel-related parts), but the potency to evoke a neurovascular response is already compromised most obviously in the supplementary motor area responsible for complex synchronizing and planning processes.

© 2012 Elsevier Inc. All rights reserved.

1. Introduction

The influence of ethanol on the brain metabolism, particularly on the neurovascular coupling, is still not fully understood. A variety of physiological mechanisms are believed to be responsible for the manifold physiological effects in the brain. Over the last few years pharmacological magnetic resonance imaging (phMRI) has been established as a powerful tool to observe pharmacological effects of drugs on neuronal activity on human as well as on animals (Honey and Bullmore, 2004; Matthews et al., 2006; Matthews, 2009; Steward et al., 2005). Thus, several groups investigated alcohol-induced effects on the neuronal activity using BOLD (blood oxygen level dependent) imaging techniques. Yoon et al. (2009) found region-dependent alterations of brain activation using memory encoding tasks. Seifritz et al. (2000) reported a BOLD signal decrease in the primary auditory cortex between 12% and 27%, depending on the definition of region of interest for signal quantitation. In order to determine the contribution of the vasodilatating effects of ethanol to potential BOLD signal changes a model calculation was performed with the conclusion that BOLD imaging should be feasible if after moderate ethanol intake the cerebral vessels have still the capacity to react appropriately on increased cerebral activity with a net increase large enough to be detected by BOLD imaging techniques. Levin et al. (1998) found that the BOLD signal amplitude was significantly reduced up to 33% in the visual cortex (VC) after ethanol application and photic stimulation. Other studies found more complex pattern of ethanol induced activation changes, depending on the brain region and the task (Calhoun et al., 2004a,b). Van Horn et al. (2006) examined the acute effects of alcohol in the context of goal-directed visuomotor performance. Sripada et al. (2011) observed the impact of ethanol regarding to fear processing. Both groups found region-dependent alterations of neuronal activity.

The underlying functional magnetic resonance imaging (fMRI) technique is based on the well known BOLD effect that provides a high temporal and spatial resolution making it ideally suited to

* Corresponding author. Tel.: +49 391 6715534; fax: +49 391 6715544.
E-mail addresses: michael.luchtmann@med.ovgu.de (M. Luchtmann), katja.jachau@med.ovgu.de (K. Jachau), daniela.adolf@med.ovgu.de (D. Adolf), friedrich-wilhelm.roehl@med.ovgu.de (F.-W. Röhl), sebastian.baecke@med.ovgu.de (S. Baecke), ralf.luetzkendorf@med.ovgu.de (R. Lützkendorf), charles.mueller@med.ovgu.de (C. Müller), johannes.bernarding@med.ovgu.de (J. Bernarding).
[1] Tel.: +49 391 6715843; fax: +49 391 6715810.
[2] Tel.: +49 391 6713535; fax: +49 391 6713536.

0161-813X/$ – see front matter © 2012 Elsevier Inc. All rights reserved.
http://dx.doi.org/10.1016/j.neuro.2012.10.017

investigate drug-induced effects on brain activity (Tank et al., 1992). BOLD fMRI is based on indirect measures of changes in regional cerebral blood flow (rCBF), regional cerebral blood volume (rCBV) as well as from alterations in the relative amount of deoxygenated hemoglobin (Ogawa et al., 1990). While it is clear that rCBF is tightly coupled to neuronal activation, the underlying coupling transduction mechanisms are still debated (Giove et al., 2003; Uludag et al., 2004). The *neurogenic hypothesis* proposes a mechanism consisting of direct innervations of blood vessels by neurons or glial cells (Iadecola, 1998; Kuschinsky and Wahl, 1978). In comparison the *metabolic hypothesis* assumes that the rCBF is changed by a release of diffusible coupling factors following the neuronal activation (Mraovitch et al., 1993; Villringer, 1997). Although the underlying physiological mechanisms are not entirely revealed, BOLD signal increases have been hypothesized to result from increased rCBF, rCBV and changes of local concentrations of deoxyhemoglobin (cerebral metabolic rate of oxygen consumption – $CMRO_2$). Furthermore it is well known that the increased rCBF following neuronal activity is much larger than the activity-induced extraction of oxygen from hemoglobin. Oxyhemoglobin and deoxyhemoglobin differ in the property to generate an extraneous magnetic field when placed in an external magnetic field. The decrease of paramagnetic deoxyhemoglobin results in greater local field homogeneities and leads to an increased MRI signal (Buxton et al., 1998). Directly after the onset of a neuronal activation the consumption of oxygen leads to a higher concentration of deoxyhemoglobin, which reduces the BOLD signal, resulting in the initial dip. The following increased rCBF and rCBV caused by neurovascular coupling lead to the above-mentioned decreased concentration of deoxyhemoglobin and thus to the typical positive BOLD response. After about 10 s following short stimulus oxygen consumption and rCBF return to their initial level. The decline of rCBF is slower. For a certain time the relative amount of deoxyhemoglobin is increased by a higher blood volume, resulting in a BOLD signal undershoot. The shape of the BOLD response following stimulation appears to be similar across early sensory and motor regions (Boynton et al., 1996; Josephs et al., 1997).

Thus, the measured BOLD signal is the sum of several signals that unfortunately cancel each other to a large extent. The effect how the individual time courses of the single components contribute to the overall BOLD signal can be seen well by simulating the curves with the balloon model (Buxton et al., 1998), which was later modified by other authors (Friston et al., 2000; Obata et al., 2004; Stephan et al., 2007; Uludag et al., 2009). Buxton et al. (1998) showed that the balloon model reproduces well the experimental BOLD data, particularly the initial dip and the post-stimulus undershoot. Friston et al. (2000) demonstrated that the balloon model is sufficient in reproducing main non-linearities observed in evoked BOLD responses. Based on the experimental work of Mandeville et al. (1999) the dynamics of the neurovascular coupling is modeled by a set of coupled non-linear differential equations describing the interaction between different physiological parameters such as neuronal activation, vessel properties, rCBF/rCBV as well as the magnetic properties of oxygenized and de-oxygenized hemoglobin that finally lead to the observable fMRI signal. The balloon model is based on two main physiological assumptions: first, the post-capillary venous compartment reacts to an increase of rCBF and rCBV like an inflating balloon. Second, the oxygen extraction is tightly coupled with the regional cerebral blood flow (Stephan et al., 2007). Although the balloon model may be over-simplistic it nevertheless may serve as a guide to analyze potential underlying processes that couple neuronal activity with vascular responses (Buxton, 2012).

However, only little is known how ethanol as one of the most prominent vessel-active drug acts on the hemodynamic response. Ethanol, which is assumed to interact with a variety of receptor systems, causes local as well as global effects (Howes and Reid, 1985; Mathew and Wilson, 1986; Stendel et al., 2006). Ethanol is also known to change the cerebral metabolism and to directly cause cerebral vasodilatation (Nicoletti et al., 2008) as well as vasoconstriction (Gordon et al., 1995).

We used the balloon model implemented in SPM8 (Stephan et al., 2007) to analyze the fMRI time series of the sensori-motor cortex and the visual cortex before and after application of moderate doses of ethanol. However, the original balloon model was customized to BOLD signals at 1.5 T magnet field strength that required adapting inherent field-dependent model parameters to 3 T (Mildner et al., 2001; Uludag et al., 2009)

To validate the results a forward simulation how parameters changes affect the BOLD-signal was performed. The analysis is based on data of a previously published study (Luchtmann et al., 2010).

2. Materials and methods

2.1. Subjects

Fourteen healthy right-handed volunteers (7 male, 7 female, aged between 21 and 29 years) were observed in a test/re-test design before and after administration of ethanol. All participants gave their written informed consent to the presented study that was approved by the Local Ethics Committee of the University of Magdeburg in compliance with national legislation and the Code of Ethical Principles for Medical Research Involving Human Subjects of the World Medical Association (Declaration of Helsinki). All volunteers were social drinkers and had experience with beverages containing high concentrations of alcohol. None of them had any self-reported history of neurological disease, major psychiatric disturbance, substance abuse, or medication usage.

2.2. Study protocol

Prior to the MRI examination the volunteers were asked to refrain from eating for 6 h and to refrain from drinking alcoholic beverages for at least 24 h. Sobriety prior to the experiment has been tested using a breath alcohol test device. All subjects were observed within an MRI scanner using BOLD imaging procedures with identical tasks prior to and after ethanol application. Ethanol-induced effects were observed using a test/re-test design. The task-framework consisted of an identical set of on/off task before and after the administration of ethanol. Therefore the time course of the BOLD signal measured under sober conditions served as baseline for potential individual ethanol effect. Between the runs under sober and alcoholic conditions all subjects had ingested a beverage containing pure ethanol mixed with 400 ml orange juice. The applied amount of ethanol to reach a blood alcohol concentration of 1.0‰ (C_o) was estimated using modified Widmark's equation:

$$C_o = \frac{a}{p \times r} \quad (1)$$

where p denotes the body weight in kg and r denotes the individual correction factor according to the equations developed by Seidl et al. (2000).

To estimate the blood alcohol concentration (BAC) the breath alcohol level (BAL) was repeatedly measured until the BAL reached about 0.8‰. For the BAL measurement a legally certified breath alcohol test device (Draeger 7110 Evidential MK III, Germany) was used. Additional blood samples were collected every 10 min. The BAC based on blood samples was measured according to the guidelines for determining blood alcohol concentration for forensic

purposes by a dehydrogenase-based enzyme assay and a gas chromatography method (Aderjan et al., 2011).

It was assumed that the BAC reached its peak level at the beginning of the second MRI session and decreases slowly thereafter. Thus, the BAC level should have been constant through the entire second MRI session.

A control group to test for placebo effects was not measured (Gensini et al., 2005). In contrast to many other placebo-controlled studies all tested participants were social drinkers and well experienced in consumption of alcoholic beverages. They knew the acute physiological effects of ethanol very well. In addition, some studies showed limited factors for the reliable use of alcohol placebos. Thus, reliable blind placebo application may only be possible when the achieved blood alcohol level is less than 0.4 ‰ (Glautier et al., 1992; Hammersley et al., 1992; Martin et al., 1990).

2.3. Experimental setting

A visually paced paradigm was used to evoke hemodynamic responses in the visual cortex (VC), the left and right primary motor cortex (LMC, RMC) as well as in the supplementary motor area (SMA). The visual stimulus consisted of a repeatedly presented checkerboard, which inverts its colors using a frequency of 8 Hz with duration of 1 s. The time between two consecutive stimuli was 19 s representing the rest condition. At this time all participants had to fixate a cross at the screen. This stimulation block was repeated 30 times every MRI session. In addition, the visual stimulus was the onset for a defined motor task comprising the successively touch of the fingers of both hands with their opposing thumb, the so-called finger-tapping task.

The entire experimental paradigm was performed twice before and after the ethanol application. For the statistical data analysis this resulted in 4 runs (2 runs for sober condition and 2 runs for ethanol condition) each of the run containing 30 blocks of 20 s duration.

2.4. MR Imaging protocol

MR imaging was performed on a 3 T Magnetom Trio scanner (Siemens, Erlangen, Germany) using a usual 8-channel phased array head coil. The conventional anatomical datasets were collected using a T1-weighted *magnetization prepared rapid gradient echo* sequence (MPRAGE – field of view = 256 mm, matrix size = 256 × 256, slices = 192, slice thickness = 1 mm).

To obtain functional datasets containing the individual hemodynamic responses a *gradient echo EPI* sequence with following parameters was used: field of view (FoV) = 192 mm, Matrix size = 64 × 64 × 7 voxel, slice thickness = 6 mm, interslice gap = 25%, Flip angle = 45°, repetition time (TR) = 500 ms, echo time (TE) = 30 ms, order of acquisition = interleaved.

2.5. Image processing and statistical analysis

The changes in neuronal activity were analyzed in a multi-step procedure using the common software packages SPM.[3] All data were preprocessed prior to the statistical analysis. All images were motion corrected to minimize the variance caused by motion artifacts. Furthermore, to facilitate a comparison across all subjects and to estimate group effects all functional datasets were normalized into a stereotactic standard space using the MNI-template. Time drifts and high frequency noise were reduced using a high-pass-filter (128 s) and the SPM built-in autoregressive model AR(1).

[3] FIL – SPM8, http://www.fil.ion.ucl.ac.uk/spm.

A design matrix containing both, the sober and ethanol condition, was modeled by convolving the stimulus duration of 1 s with the standard SPM canonical HRF (hemodynamic response function). To account for the variability in the hemodynamic response across the sober and ethanol condition the design matrix was extended by the derivatives of the HRF, with respect to time and dispersion. Inferences about cerebral activations were made using *F*- and *t*-contrasts (Friston et al., 1994, 1995; Worsley and Friston, 1995).

Finally, the hemodynamic parameters were estimated for each region and condition. Significantly activated clusters (family wise error, $p < 0.001$) of the above-mentioned regions VC, RMC, LMC and SMA served as regions of interest.

To investigate the underlying vascular und metabolic contributions of the ethanol-induced changes in BOLD signal the balloon model (Buxton et al., 1998), implemented und modified in SPM8 was used. The model parameters in SPM8 were estimated for 1.5 T. Assuming, that two parameters (ν_0, the ratio of the intra- to the extravascular signal, and r_0, the slope of the relation between the intravascular relaxation rate $R^*_{2\,\mathrm{intravasc}}$ and oxygen saturation) should exhibit to first order a linear dependency from the B_0 field we adapted these parameters in the source code of SPM8 (spm_gx_hdm.m) prior to applying the balloon model analysis. Thus, these values were doubled to $\nu_0 = 80.6\ \mathrm{s}^{-1}$ and $r_0 = 50\ \mathrm{s}^{-1}$.

To test the parameters for significant changes a two-factorial analysis of variance was used to reveal global influence of ethanol on any balloon model parameter. Here, a Huynh–Feldt correction was used for multiple adjustments. The explorative post hoc analysis of all parameters across all regions and conditions was calculated using a two-tailed paired *t*-test (Bonferroni corrected).

2.6. Balloon model simulation

For estimating potential ethanol-induced changes of the components determining neurovascular coupling, the balloon model (Buxton et al., 1998; Friston et al., 2000; Deneux and Faugeras, 2006; Stephan et al., 2007) provides a well-established model that gives insight into the interdependencies between the underlying mechanisms and how changing them affects the resulting BOLD signal.

The balloon model describes an input-output model which is characterized by two state variables: output volume $\nu(t)$ and deoxyhemoglobin content $q(t)$. The input to this system is represented by the blood inflow $f(t)$. The BOLD signal is assumed to be a combination of many neurogenic and diffusive signal subcomponents. For this, the model comprises a set of parameters that exert influence on the dynamics of the hemodynamic response and thus on the temporal time course of the BOLD signal. The parameter S_e represents the relationship between neuronal activity and the resulting neuronal signal. This connection was originally called *neuronal efficacy* and labeled as epsilon (Friston et al., 2000). However, this may lead to confusion with the parameter epsilon describing the ratio between intra- to extravascular signal, which was introduced in a newer version of SPM (Stephan et al., 2007). SPM8 also uses the expression *stimulus efficacy* instead of neuronal efficacy in a more comprehensive context of coupled activated areas. For a separated analysis of activated regions as performed here both expressions should represent the same dependence between neuronal activation and induced vascular flow signal. The according signal induces a change of the inflowing blood $f(t)$. *Signal decay* describes the time-constant how this signal decreases when the neuronal induction ceases. The parameter *feedback* represents the time-constant for the vessel-based autoregulatory mechanisms the counteract

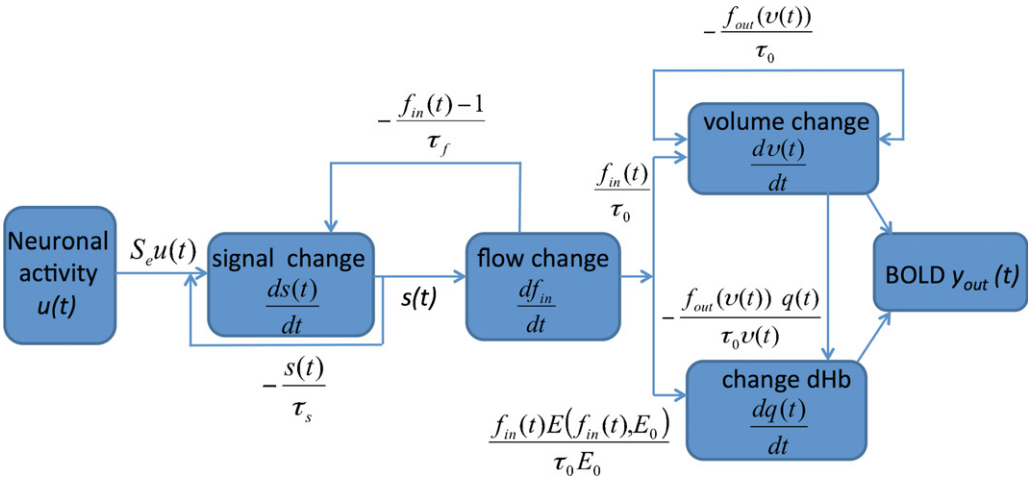

Fig. 1. Schematic illustration of the balloon model (details are described in the main text).

alterations of the blood flow. The *transit time* is the average time necessary to traverse the venous compartment. The parameter *exponent* describes the stiffness of the flow-volume relationship of the venous balloon. *Oxygen extraction* is the resting net oxygen extraction fraction within the capillary bed. Finally, the dynamics of the changes in hemoglobin oxygenation and the venous volume are combined to yield the BOLD signal. The according weighting factors however depend on additional parameters, most importantly on the external magnetic field and thus subsequently on the susceptibility effects between the intra- and extravascular signals.

The above dynamics are modeled by a set of coupled non-linear equations (Buxton et al., 1998; Mandeville et al., 1999; Friston et al., 2000; Stephan et al., 2007).

The model (see Fig. 1) assumes that the neuronal activation $u(t)$ triggers with a certain efficacy ε a cascade of metabolic mechanisms that ultimately generate a signal $s(t)$ that induces finally a change of the inflow $f_{\text{in}}(t)$ into the activated area:

$$s(t) = \frac{d f_{\text{in}}}{dt} \tag{2}$$

Due to feedback mechanisms the increase of the flow-inducing signal $s(t)$ decays proportional to the signal itself (with a rate τ_s) and with a rate τ_f due to a negative feedback (the so-called autoregulation) which is correlated to the induced flow $f_{\text{in}}(t)$:

$$\frac{ds(t)}{dt} = \varepsilon u(t) - \frac{s(t)}{\tau_s} - \frac{f_{\text{in}}(t) - 1}{\tau_f} \tag{3}$$

In the original balloon model the BOLD signal $y(t)$ is composed by the contributions of the venous blood volume $v(t)$ and the concentration $q(t)$ of de-oxyhemoglobine (dHB) weighted by constants k_i according to

$$y(t) = V_0(k_1(1 - q(t)) + k_2\left(1 - \frac{q(t)}{v(t)}\right) + k_3(1 - v(t)) \tag{4}$$

The functions $q(t)$ and $v(t)$ are coupled to the inflow signal through

$$\tau_0 \frac{dv(t)}{dt} = f_{\text{in}}(t) - f_{\text{out}}(v(t)), \quad f_{\text{out}}(v(t)) = v(t)^{1/\alpha} \tag{5}$$

$$\tau_0 \frac{dq(t)}{dt} = \frac{f_{\text{in}}(t)E(f_{\text{in}}(t), E_0)}{E_0} - \frac{f_{\text{out}}(v(t))q(t)}{v(t)} \tag{6}$$

$$E(f_{\text{in}}(t), E_0) = 1 - (1 - E_0)^{f_{\text{in}}(t)} \tag{7}$$

The original parameters $k_1 = 7E_0$, $k_2 = 2$, $k_3 = 2E_0 - 0.2$ were adapted according to Stephan et al. (2007) to

$$\begin{aligned} k_1 &= 4.3\nu_0 E_0\,\text{TE}, \\ k_2 &= \varepsilon r_0 E_0\,\text{TE}, \\ k_3 &= 1 - \varepsilon, \end{aligned} \tag{7a}$$

where TE is the echo time, ν_0 is the frequency offset at the outer surface of the magnetized vessel for fully deoxygenated blood, E_0 is the oxygen extraction at rest, e is the ratio of intra- to extravascular signal, and r_0 is the slope of the relation between the intravascular relaxation rate and oxygen saturation.

The hemodynamic response functions were calculated according to the modified balloon model (Stephan et al., 2007). The system of non-linear differential equations was implemented in Maple11.[4] Simulation parameters according to the nomenclature of Stephan et al. (2007) were: activation duration 1 s, amplitude of neuronal activation 1.0, signal decay $\tau_s = 1.83$ s, autoregulation $\tau_f = 1.85$ s, transit time $\tau_0 = 2.2$ s, oxygen extraction rate $E_0 = 0.48$, Grubbs constant $\alpha = 0.45$, $V_0 = 0.02$, ratio of intravascular and extravascular signal $\varepsilon = 0.49$. TE was set to 30 ms according to the experimental setup.

3. Results

A mean BAC of 0.82 ± 0.07‰ was measured across all fourteen subjects. No significant changes were detected during the entire experiment under the ethanol condition.

The baseline and corresponding hemodynamic responses of each region were averaged across all subjects. No significant changes were detected in the mean baseline after the ethanol application ($p = 0.131$).

3.1. General linear model using SPM8

The results of the random-effects analysis for the conditions *sober* and *ethanol* using SPM are shown in Figs. 2 and 3. The paradigm reliably evoked the regions LMC, RMC, SMA and VC before as well as after ethanol digestion.

3.2. Analysis of balloon model parameters

Across all subjects, regions and conditions the hemodynamic BOLD parameters were estimated based on the modified balloon

[4] Maple 11, Waterloo Maple, Inc., http://www.maplesoft.com.

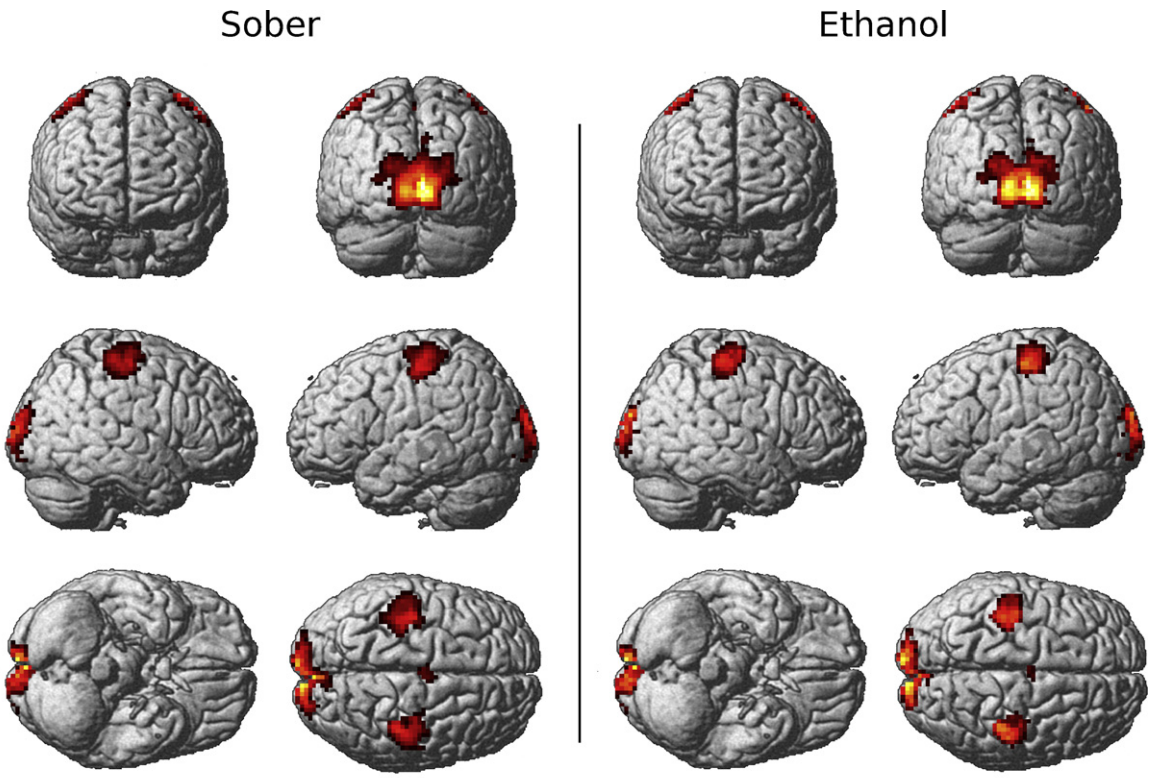

Fig. 2. Results of the main effects of the random effects analysis using SPM. The activation-maps of the group-level analysis across all 14 subjects are shown. The observed regions LMC, RMC, SMA and VC exhibit a significant BOLD-activity for the sober and the ethanol condition ($p < 0.01$, family wise error (FWE) corrected).

model by Stephan et al. (2007) implemented in SPM8. Table 1 shows the results of a two-factorial analysis of variance. The parameters *stimulus efficacy* and *transit time* were significantly influenced by the effect of ethanol. Region-dependent changes were shown for all observed parameters but only the parameters *transit time* and *stimulus efficacy* exhibit a trend to show different ethanol dependent influence across the explored regions.

Table 2 shows the results of the explorative-post hoc analysis of the balloon model parameter estimation. The parameter *transit time* was significantly increased after ethanol consumption across all observed regions. The smallest increase was found in the supplementary motor area, the largest in the visual cortex. The parameter *stimulus efficacy*, however, showed an ethanol-induced decrease across all observed regions. The mean decrease was by about a third in left and right primary motor cortex and the visual cortex. The most significant reduction of the *stimulus efficacy* was seen in the SMA. All analysis of all other parameters yielded no significant ethanol-induced effects.

3.3. Balloon model simulations

The interaction of the different parameters of the balloon model is complex and their effects may cancel each other. Therefore, different parameter combinations may account for a similar BOLD signal. However, the model provides an apt basis for examining the effect of the parameter changes. To verify how changes in the parameters affect the BOLD signal the according signals were simulated by independently varying the parameters (Fig. 4a and b). The reduction in neuronal activation leads to a corresponding reduction of the amplitude of the BOLD signal but does neither increase the full-width-at-half-maximum (FWHM) nor shift the post-stimulus undershoot toward positive values as observed in the experiments. The increase in τ_f (autoregulation) increases both the amplitude and the FWHM while increasing time-to-peak (TTP) only slightly. Increasing the transit time τ_0 prolongs TTP more clearly and additionally decreases the amplitude (Fig. 4b) albeit less than the reduction of the stimulus efficacy. A similar effect is seen by increasing the vessel stiffness (Grubbs constant a) but additionally a profound deepening of the initial dip results. The signal was fairly insensitive to changes in r_0 within the range of 20%.

4. Discussion

To our knowledge this is the first study to evaluate the impact of ethanol on the neurovascular coupling using the well-known balloon model (Buxton et al., 1998).

Interestingly, only two of the parameters showed a significant change after application of ethanol. All observed regions exhibited a clear decrease of the *stimulus efficacy*. The two-factorial analysis of variance showed a trend toward region-dependent influence of ethanol on the stimulus efficacy. The differences in the reduction of the parameter *stimulus efficacy* across the observed regions may support the assumption that ethanol has a region dependent impact on the neuronal activity (Van Horn et al., 2006). Compared

Table 1
Results (p-values, Huynh–Feldt corrected) of the two-factorial analysis of variance to discover global effects in the balloon parameter approximation.

Parameter	Factor		
	Ethanol	Region	Ethanol × region
Stimulus efficacy	0.0013	<0.0001	0.0723
Signal decay	0.5357	<0.0001	0.8412
Feedback	0.8763	0.0004	0.3695
Transit time	0.0006	<0.0001	0.0707
Exponent	0.4394	<0.0001	0.6183
Extraction	0.5769	<0.0001	0.9555

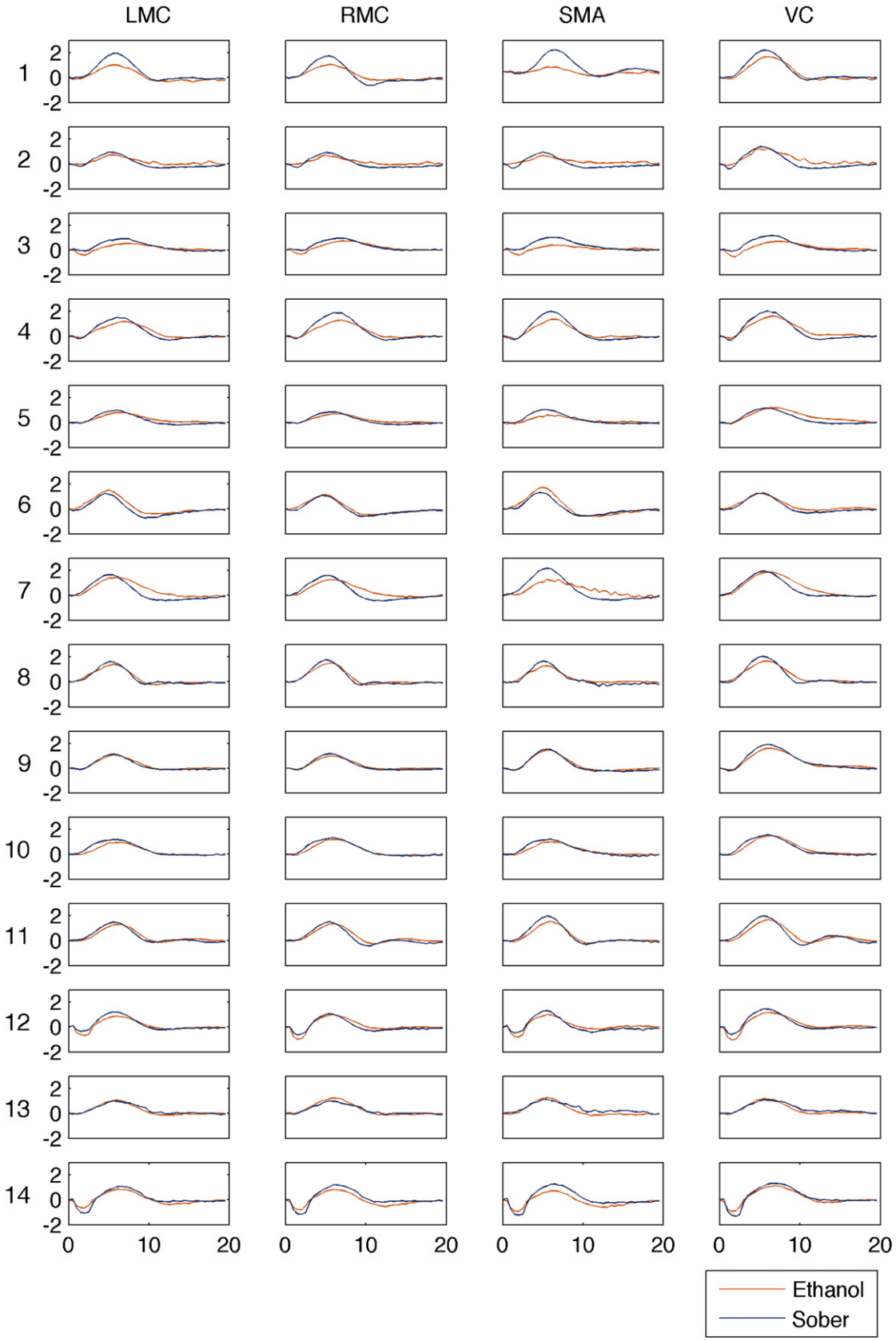

Fig. 3. Individual hemodynamic responses before (blue) and after (orange) application of ethanol. (For interpretation of the references to color in this figure legend, the reader is referred to the web version of the article.)

Table 2
Results (Bonferroni corrected) of the explorative analysis of the balloon model hemodynamic parameter using a two-tailed paired *t*-test (significant results are depicted bold face – signal decay [1/s], feedback [1/s], transit time [s], extraction [%]).

	Sober	Ethanol	Difference	Diff. %	*p*-Value
Left motor cortex (LMC)					
Stimulus efficacy	0.179 ± 0.09	0.116 ± 0.08	−0.063 ± 0.06	−35.19	**0.010**
Signal decay	0.702 ± 0.46	0.704 ± 0.46	0.002 ± 0.07	0.28	0.999
Feedback	0.365 ± 0.03	0.371 ± 0.08	0.006 ± 0.04	1.64	0.999
Transit time	1.205 ± 0.23	1.432 ± 0.19	0.227 ± 0.20	18.84	**0.002**
Exponent	0.326 ± 0.01	0.326 ± 0.01	0.000 ± 0.01	0.00	0.999
Extraction	35.00 ± 0.84	34.93 ± 0.80	−0.07 ± 3.86	−0.19	0.999
Right motor cortex (RMC)					
Stimulus efficacy	0.191 ± 0.07	0.130 ± 0.08	−0.061 ± 0.07	−31.94	**0.014**
Signal decay	0.706 ± 0.04	0.707 ± 0.04	0.001 ± 0.04	0.14	0.999
Feedback	0.362 ± 0.03	0.369 ± 0.02	0.007 ± 0.04	1.93	0.999
Transit time	1.259 ± 0.20	1.459 ± 0.21	0.200 ± 0.19	15.89	**0.005**
Exponent	0.327 ± 0.01	0.325 ± 0.01	−0.002 ± 0.01	−0.61	0.755
Extraction	35.27 ± 0.88	35.07 ± 0.70	−0.20 ± 1.08	−0.57	0.999
Supplementary motor area (SMA)					
Stimulus efficacy	0.155 ± 0.06	0.086 ± 0.05	−0.069 ± 0.04	−44.52	**0.001**
Signal decay	0.676 ± 0.02	0.680 ± 0.02	0.004 ± 0.03	0.59	0.999
Feedback	0.383 ± 0.02	0.385 ± 0.01	0.002 ± 0.02	0.52	0.999
Transit time	1.144 ± 0.16	1.128 ± 0.14	0.140 ± 0.13	12.24	**0.005**
Exponent	0.326 ± 0.01	0.323 ± 0.00	−0.003 ± 0.01	−0.92	0.657
Extraction	34.80 ± 0.77	34.60 ± 0.74	−0.20 ± 0.77	−0.58	0.999
Visual cortex (VC)					
Stimulus efficacy	0.353 ± 0.01	0.225 ± 0.13	−0.129 ± 0.16	−36.54	**0.026**
Signal decay	0.720 ± 0.06	0.736 ± 0.07	0.016 ± 0.08	2.22	0.999
Feedback	0.355 ± 0.04	0.347 ± 0.05	−0.008 ± 0.05	−2.25	0.999
Transit time	1.390 ± 0.39	1.665 ± 0.76	0.275 ± 0.29	19.78	**0.011**
Exponent	0.332 ± 0.01	0.331 ± 0.01	−0.001 ± 0.01	−0.30	0.999
Extraction	35.73 ± 1.22	35.60 ± 1.18	−0.13 ± 1.19	−0.36	0.999

to the regions LMC, RMC and VC the SMA showed a higher susceptibility to ethanol. This result is consistent with the assumption that ethanol has an influence on specific cerebral receptor systems (Allan et al., 1987; Allan and Harris, 1986; Davies, 2003). Geyer et al. (1998) showed an increased density of $GABA_A$ (gamma-aminobutyric acid) binding sites in the SMA that play an important role in mediating ethanol induced effects. The binding of ethanol to $GABA_A$ receptors results in an inhibition of the neuron and may lead therefore to a decreased neuronal activity expressed in the balloon model as a decreased event density. The parameter *signal decay* reflects the transduction of neuronal activity into changes in rCBF. At spatial scales of several millimeters it is likely that rapidly diffusing molecules like nitric oxide mediate increases in rCBF through the relaxation of smooth muscle cells in the arteriolar wall (Stephan et al., 2007). No significant changes of this parameter were shown following the ethanol digestion. These results may lead to the conclusion that ethanol does not alter the sensitivity for nitric oxide (NO). Mayhan et al. (1995) suggest that acute exposure of cerebral arterioles to moderate doses ethanol does not alter the hemodynamic responses to nitric oxide. Toda and Ayajiki (2010) even showed an increased NO production following low dose application of ethanol. An increased NO production under the condition of an unchanged sensitivity for nitric oxide may lead to an increased cerebral blood flow, which was shown by recent studies of Rickenbacher et al. (2011). The parameter *feedback* is a time-constant of cerebral autoregulatory mechanism. It represents the concept of cerebral vasodilatating vessel properties in terms of blood flow constancy during perfusion pressure changes (Paulson et al., 1990). In no region significant changes of the parameter *feedback* were found. These findings imply that cerebral vessels possess robust mechanisms to prevent ethanol-induced impairment of autoregulatory mechanisms. These findings are in line with the results of another study. Thus, Blaha et al. (2003) observed the effects of acute alcohol intoxication on the dynamic cerebral autoregulation directly using transcranial Doppler. It has been shown that the dynamic cerebral autoregulation was not significantly impaired by moderate doses of ethanol across wide ranges of blood pressures (Blaha et al., 2003). Grubb et al. (1974) described the flow out of the venous compartment that models the balloon-like capacity as a function of blood volume. According to Mandeville et al. (1999) this outflow is strongly characterized by Grubbs constant (see Table 2, parameter *exponent*). No ethanol-induced changes were found for the parameter *exponent* across all observed regions. Besides the *stimulus efficacy* only the *transit time* was significantly altered. As the transit time measures the time that a blood cell takes to transverse the venous compartment during stimulation the prolongation of the mean *transit time* indicates a slow down of the dynamics of the BOLD signal with respect to the flow changes. The results of the balloon-model-based analysis using SPM8 show this significant increase of the *transit time* across all observed regions under ethanol condition. These results are inconsistent with the findings of Blaha et al. (2003), who showed an increase of the cerebral blood flow velocity (CBFV) in the middle cerebral arteries (MCA) up to 8% following an ethanol application. In contrast to the results of Blaha et al. (2003) an increase of the parameter *transit time* was found indicating a decreased CBFV. At similar levels of BAC the differences of the changes of the CBFV may be explained by methodical reasons. While the balloon model in the present study considers the venous compartment of the capillary bed Blaha et al. (2003) measured the CBF of arteries (MCA). The parameter *extraction* describes the resting net oxygen extraction of the capillary bed. The estimation of this parameter shows a mean extraction fraction of about 35% for both the sober and the ethanol condition. Thus, the values were within the known physiological range between 20% and 50% (Friston et al., 2000). The statistical analysis of the alcohol-induced changes of the net resting oxygen extraction, described by the parameter *extraction*, exhibited no significant changes after the ethanol digestion. Assuming constant arterial oxygen saturation the results led to an

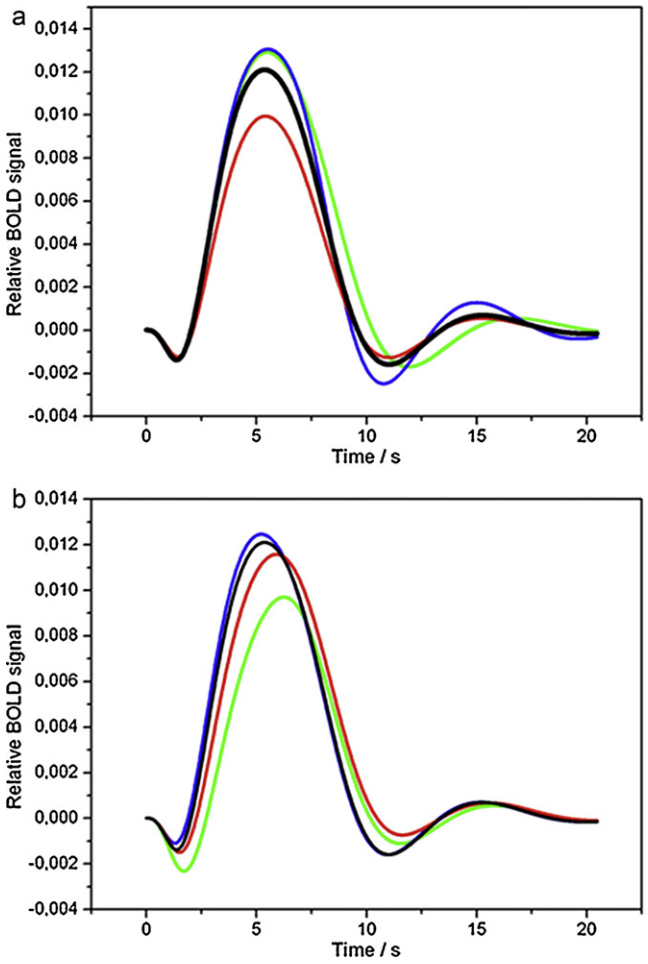

Fig. 4. Alteration of the BOLD signal as a function of changing the parameter of the modified balloon model separately. The black curve represents a fit to a representative BOLD signal of the present study. (a) Red curve = 20% reduction in neuronal activation; blue curve = 20% increase in τ_s; green curve = 20% increase in τ_f. (b) Red curve = 20% increase in τ_0; blue curve = 20% increase in ε (ratio between intravascular and extravascular signal); green curve = 20% increase in Grubbs constant a. (For interpretation of the references to color in this figure legend, the reader is referred to the web version of the article.)

unchanged cerebral oxygen extraction ratio. These findings are contrary to the observations of Zink et al. (1998a,b). They studied the effects of ethanol in a model of combined traumatic brain injury and hemorrhagic shock using iatrogenic brain injured pigs. A significant increase of the cerebral oxygen extraction ratio was found following the intragastric ethanol application. The following metabolic and structural alteration of the brain may explain the contrary results. Thus, Ibayashi et al. (2000) observed in patients with chronic ischemic stroke an increased oxygen extraction fraction indicating the brain to be in a metabolically ischemic state or increased anaerobic glycolysis with oxygen. In contrast to the study conducted by Ibayashi et al. (2000) the participants of the present examination were clinically healthy. Therefore, a direct comparison is not useful.

The influence of ethanol on the brain metabolism, particularly on the neurovascular coupling, is still not fully understood. A variety of molecular mechanisms are believed to be responsible for the manifold physiological effects in the brain. Some studies claim that ethanol stimulates adenylate cyclase activity by modifying the regulatory G-protein–adenylate cyclase interaction to increase the production of activated enzymes. This action is supposed to be additive with the effects of dopamine on adenylate cyclase (Hoffman and Tabakoff, 1990; Hoffman et al., 1984). Additionally, ethanol leads to changes in adrenergic receptor systems in the brain. In vitro it has been shown that ethanol decreases the affinity of the high-affinity state of the receptor for isoproterenol (Hoffman et al., 1987; Valverius et al., 1987). In recent years $GABA_A$ receptors occupy a central role in mediating the effects of ethanol in mammalian brain. A large body of evidence is showing that $GABA_A$ receptors are responsible for both the short and the long-term effects of ethanol in the central nervous system (Davies, 2003). The binding of ethanol to the $GABA_A$ receptors increases the influx of chloride ions through the cell membrane and leads to an inhibition of new action potentials. Thus, the binding of $GABA_A$ receptor agonists results in an inhibition of the neuron. Allan et al. (1987) and Allan and Harris (1986) show the direct augmentation of the chloride ion influx of $GABA_A$ receptors after ethanol exposure. The presented results are consistent with the studies of Geyer et al. (1998). The regional distributions of $GABA_A$ binding sites were analyzed in the motor area of the macaque mesial frontal cortex across the regions F1, F3 and F6. These regions are homologous to the primary motor cortex (F1), the caudal (F3) and the rostral SMA (F6) in the human brain. It has been shown that the density of $GABA_A$ receptors in the SMA is up to 35% higher compared to the primary motor cortex. The results of our study imply that ethanol has a stronger impact on the SMA than on the primary motor and visual cortex. Thus, the presented results support the claim that the $GABA_A$ receptor has a central role in mediating the short-term effects of ethanol.

4.1. Balloon model simulations

Forward simulations supported the results of the analysis. These showed, similar to results of Friston et al. (2000), that isolated parameter changes affect the BOLD signal partly opposite with regard to initial dip, time-to-peak, FWHM, and undershoot. However, these complex changes exhibit characteristic patterns. The isolated decrease of neuronal activity leads to a decreased BOLD amplitude, which was also the first main result of the balloon-model analysis. Similarly, the prolongation of the transit time leads to a significant increase of the TTP. However, it has to be kept in mind that the complex non-linear behavior of the differential equations may allow other solutions that are characterized by local minima in the model space. We also assumed that v_0 and r_0 scale linearly with the external magnetic field. This led to the same biophysiological constants used by Mildner et al. (2001). However, in the SPM8 implementation k_2 and k_3 both contain the parameter ε (ratio of intra- to extravascular signal) as a free fit parameter which renders the comparison to the k_2 and k_3 in the formulation of Mildner et al. (2001) somewhat difficult.

Although the results of the analysis have to be interpreted therefore with caution extended tests and comparisons of different models (Deneux and Faugeras, 2006) showed that the model may be used as a starting point for describing the mechanisms underlying the BOLD signal. A recent review on modeling the BOLD signal was published by Buxton who discusses the limitations of the balloon model and the development of more sophisticated models (Buxton, 2012) especially concerning the BOLD characteristics in higher fields (Uludag et al., 2009).

5. Conclusion

Examining the impact of drugs affecting the neuro-vascular coupling such as ethanol leads to complex alterations of the hemodynamic response function, which depend on the cortical region. Analysing the fMRI time series based on a set of non-linear differential equations based on the balloon model showed that the main effect was a reduction of the stimulus efficacy and a

prolongation of the transit time. One may therefore assume, that at the moderate alcohol levels applied in this study the capability of the neurons to evoke a hemodynamic signal cascade is compromised. However, once initiated that chain of processes seems to be rather intact as seen for the unchanged vessel and signal feedback parameters. There is enough vascular reserve to lead to a vessel-based response albeit the transit time is somewhat reduced Instead. The analysis suggests that the main effect of ethanol may be localized on the neuronal level or in the capability of the neurons to translate activation into another signal cascade ultimately leading to increased oxygen supply. Our results are in line with the assumption that inhibiting $GABA_A$ receptors play a crucial role in meditating ethanol-induced short-term effects.

However, a word of caution applies for using the model for BOLD signal changes. The finally detected fMRI signal is composed by several components that mutually cancel each other. Accordingly, the space of solutions has many possible parameter combinations therefore the priors used in fitting the curves have to be chosen quite reasonably. But the obvious clear-cut changes as in the above analysis support strongly the interpretation that the model may give insight into underlying mechanisms. It would be interesting to increase the dose of ethanol and to investigate other cortical areas that may be more sensitive to ethanol than the motor region.

Conflict of interest statement

The authors declare that there are no conflicts of interest.

References

Aderjan R, Daldrup T, Käferstein H, Krause D, Mubßhoff F, Paul LD, et al. Guidelines for determining blood alcohol concentration (BAC) for forensic purposes – BAC guidelines. Blutalkohol 2011;48(3):137–43.

Allan AM, Huidobro-Toro JP, Bleck V, Harris RA. Alcohol and the GABA receptor-chloride channel complex of brain. Alcohol Alcohol (Suppl. 1):1987;643–6.

Allan AM, Harris RA. Gamma-aminobutyric acid and alcohol actions: neurochemical studies of long sleep and short sleep mice. Life Sci 1986;39(21):2005–15.

Blaha M, Aaslid R, Douville CM, Correra R, Newell DW. Cerebral blood flow and dynamic cerebral autoregulation during ethanol intoxication and hypercapnia. J Clin Neurosci 2003;10(2):195–8.

Boynton GM, Engel SA, Glover GH, Heeger DJ. Linear systems analysis of functional magnetic resonance imaging in human V1. J Neurosci 1996;16(13):4207–21.

Buxton RB. Dynamic models of BOLD contrast. Neuroimage 2012;62(2):953–61.

Buxton RB, Wong EC, Frank LR. Dynamics of blood flow and oxygenation changes during brain activation: the balloon model. Magn Reson Med 1998;39(6):855–64.

Calhoun VD, Pekar JJ, Pearlson GD. Alcohol intoxication effects on simulated driving: exploring alcohol-dose effects on brain activation using functional MRI. Neuropsychopharmacology 2004;29(11):2097–107.

Calhoun VD, Altschul D, McGinty V, Shih R, Scott D, Sears E, et al. Alcohol intoxication effects on visual perception: an fMRI study. Hum Brain Mapp 2004;21(1):15–25.

Davies M. The role of GABAA receptors in mediating the effects of alcohol in the central nervous system. J Psychiatry Neurosci 2003;28(4):263–74.

Deneux T, Faugeras O. Using nonlinear models in fMRI data analysis: model selection and activation detection. Neuroimage 2006;32(4):1669–89.

Friston KJ, Mechelli A, Turner R, Price CJ. Nonlinear responses in fMRI: the balloon model, volterra kernels, and other hemodynamics. Neuroimage 2000;12(4):466–77.

Friston KJ, Holmes AP, Poline J, Grasby PJ, Williams SCR, Frackowiak RSJ, et al. Analysis of fMRI time-series revisited. Neuroimage 1995;2(1):45–53.

Friston KJ, Holmes AP, Worsley KJ, Poline J, Frith CD, Frackowiak RSJ. Statistical parametric maps in functional imaging: a general linear approach. Hum Brain Mapp 1994;2(4):189–210.

Gensini GF, Conti AA, Conti A. Past and present of "what will please the lord": an updated history of the concept of placebo. Minerva Med 2005;96(2):121–4.

Geyer S, Matelli M, Luppino G, Schleicher A, Jansen Y, Palomero-Gallagher N, et al. Receptor autoradiographic mapping of the mesial motor and premotor cortex of the macaque monkey. J Comp Neurol 1998;397(2):231–50.

Giove F, Mangia S, Bianciardi M, Garreffa G, Di Salle F, Morrone R, et al. The physiology and metabolism of neuronal activation: in vivo studies by NMR and other methods. Magn Reson Imaging 2003;21(10):1283–93.

Glautier S, Remington B, Taylor C. Alcohol placebos: you can only fool some of the people some of the time [2]. Br J Addict 1992;87(10):1489.

Gordon EL, Nguyen T-. Ngai AC, Winn HR. Differential effects of alcohols on intracerebral arterioles. Ethanol alone causes vasoconstriction. J Cereb Blood Flow Metab 1995;15(3):532–8.

Grubb RL Jr, Raichle ME, Eichling JO, Ter Pogossian MM. The effects of changes in $PaCO_2$ on cerebral blood volume, blood flow, and vascular mean transit time. Stroke 1974;5(5):630–9.

Hammersley R, Finnigan F, Millar K. Alcohol placebos: you can only fool some of the people all of the time. Br J Addict 1992;87(10):1477–80.

Hoffman PL, Tabakoff B. Ethanol and guanine nucleotide binding proteins: a selective interaction. FASEB J 1990;4(9):2612–22.

Hoffman PL, Valverius P, Kwast M, Tabakoff B. Comparison of the effects of ethanol on beta-adrenergic receptors in heart and brain. Alcohol Alcohol (Suppl. 1):1987;749–54.

Hoffman PL, Luthin GR, Theodoropoulos D. Ethanol effects on striatal dopamine receptor-coupled adenylate cyclase and on striatal opiate receptors. Pharmacol Biochem Behav 1984;18(Suppl. 1):355–9.

Honey G, Bullmore E. Human pharmacological MRI. Trends Pharmacol Sci 2004;25(7):366–74.

Howes LG, Reid JL. Decreased vascular responsiveness to noradrenaline following regular ethanol consumption. Br J Clin Pharmacol 1985;20(6):669–74.

Iadecola C. Neurogenic control of the cerebral microcirculation: is dopamine minding the store? Nat Neurosci 1998;1(4):263–5.

Ibayashi S, Irie K, Kitayama J, Nagao T, Kitazono T, Fujishima M. Ischemic brain metabolism in patients with chronic cerebrovascular disease: increased oxygen extraction fraction and cerebrospinal fluid lactate. J Stroke Cerebrovasc Dis 2000;9(4):166–71.

Josephs O, Turner R, Friston K. Event-related fMRI. Hum Brain Mapp 1997;5(4):243–8.

Kuschinsky W, Wahl M. Local chemical and neurogenic regulation of cerebral vascular resistance. Physiol Rev 1978;58(3):656–89.

Levin JM, Ross MH, Mendelson JH, Kaufman MJ, Lange N, Maas LC, et al. Reduction in BOLD fMRI response to primary visual stimulation following alcohol ingestion. Psychiatr Res – Neuroimaging 1998;82(3):135–46.

Luchtmann M, Jachau K, Tempelmann C, Bernarding J. Alcohol induced region-dependent alterations of hemodynamic response: implications for the statistical interpretation of pharmacological fMRI studies. Exp Brain Res 2010;1–10.

Mandeville JB, Marota JJA, Ayata C, Zaharchuk G, Moskowitz MA, Rosen BR, et al. Evidence of a cerebrovascular postarteriole windkessel with delayed compliance. J Cereb Blood Flow Metab 1999;19(6):679–89.

Martin CS, Earleywine M, Finn PR, Young RD. Some boundary conditions for effective use of alcohol placebos. J Stud Alcohol 1990;51(6):500–5.

Mathew RJ, Wilson WH. Regional cerebral blood flow changes associated with ethanol intoxication. Stroke 1986;17(6):1156–9.

Matthews PM. Pharmacological applications of fMRI. Neuromethods 2009;41:751–67.

Matthews PM, Honey GD, Bullmore ET. Applications of fMRI in translational medicine and clinical practice. Nat Rev Neurosci 2006;7(9):732–44.

Mayhan WG, Didion SP, Wei EP. Acute effects of ethanol on responses of cerebral arterioles. Stroke 1995;26(11):2097–102.

Mildner T, Norris DG, Schwarzbauer C, Wiggins CJ. A qualitative test of the balloon model for BOLD-based MR signal changes at 3 T. Magn Reson Med 2001;46(5):891–9.

Mraovitch S, Calando Y, Onteniente B, Peschanski M, Seylaz J. Cerebrovascular and metabolic uncoupling in the caudate-putamen following unilateral lesion of the mesencephalic dopaminergic neurons in the rat. Neurosci Lett 1993;157(2):140–4.

Nicoletti P, Trevisani M, Manconi M, Gatti R, De Siena G, Zagli G, et al. Ethanol causes neurogenic vasodilation by TRPV1 activation and CGRP release in the trigeminovascular system of the guinea pig. Cephalalgia 2008;28(1):9–17.

Obata T, Liu TT, Miller KL, Luh W-. Wong EC, Frank LR, et al. Discrepancies between BOLD and flow dynamics in primary and supplementary motor areas: application of the balloon model to the interpretation of BOLD transients. Neuroimage 2004;21(1):144–53.

Ogawa S, Lee TM, Kay AR, Tank DW. Brain magnetic resonance imaging with contrast dependent on blood oxygenation. Proc Natl Acad Sci U S A 1990;87(24):9868–72.

Paulson OB, Strandgaard S, Edvinsson L. Cerebral autoregulation. Cerebrovasc Brain Metab Rev 1990;2(2):161–92.

Rickenbacher E, Greve DN, Azma S, Pfeuffer J, Marinkovic K. Effects of alcohol intoxication and gender on cerebral perfusion: an arterial spin labeling study. Alcohol 2011;45(8):725–37.

Seidl S, Jensen U, Alt A. The calculation of blood ethanol concentrations in males and females. Int J Legal Med 2000;114(1–2):71–7.

Seifritz E, Bilecen D, Hänggi D, Haselhorst R, Radü EW, Wetzel S, et al. Effect of ethanol on BOLD response to acoustic stimulation: implications for neuropharmacological fMRI. Psychiatr Res – Neuroimaging 2000;99(1):1–13.

Sripada CS, Angstadt M, McNamara P, King AC, Phan KL. Effects of alcohol on brain responses to social signals of threat in humans. Neuroimage 2011;55(1):371–80.

Stephan KE, Weiskopf N, Drysdale PM, Robinson PA, Friston KJ. Comparing hemodynamic models with DCM. Neuroimage 2007;38(3):387–401.

Stendel R, Irnich B, al Hassan AA, Heidenreich J, Pietilae T. The influence of ethanol on blood flow velocity in major cerebral vessels. A prospective and controlled study. Alcohol 2006;38(3):139–46.

Steward CA, Marsden CA, Prior MJW, Morris PG, Shah YB. Methodological considerations in rat brain BOLD contrast pharmacological MRI. Psychopharmacology (Berl) 2005;180(4):687–704.

Toda N, Ayajiki K. Vascular actions of nitric oxide as affected by exposure to alcohol. Alcohol Alcohol 2010;45(4):347–55.

Tank DW, Ogawa S, Ugurbil K. Mapping the brain with MRI. Curr Biol 1992;2(10):525–8.

Uludag K, Dubowitz DJ, Yoder EJ, Restom K, Liu TT, Buxton RB. Coupling of cerebral blood flow and oxygen consumption during physiological activation and deactivation measured with fMRI. Neuroimage 2004;23(1):148–55.

Uludag K, Müller-Bierl B, U?urbil K. An integrative model for neuronal activity-induced signal changes for gradient and spin echo functional imaging. Neuroimage 2009;48(1):150–65.

Valverius P, Hoffman PL, Tabakoff B. Effect of ethanol on mouse cerebral cortical β-adrenergic receptors. Mol Pharmacol 1987;32(2):217–22.

Van Horn JD, Yanos M, Schmitt PJ, Grafton ST. Alcohol-induced suppression of BOLD activity during goal-directed visuomotor performance. Neuroimage 2006;31(3):1209–21.

Villringer A. Understanding functional neuroimaging methods based on neurovascular coupling. Adv Exp Med Biol 1997;413:177–93.

Worsley KJ, Friston KJ. Analysis of fMRI time-series revisited – again. Neuroimage 1995;2(3):173–81.

Yoon HW, Chung J, Oh J, Min H, Kim D, Cheon Y, et al. Differential activation of face memory encoding tasks in alcohol-dependent patients compared to healthy subjects: an fMRI study. Neurosci Lett 2009;450(3):311–6.

Zink BJ, Sheinberg MA, Wang X, Mertz M, Stern SA, Betz AL. Acute ethanol intoxication in a model of traumatic brain injury with hemorrhagic shock: effects on early physiological response. J Neurosurg 1998;89(6):983–90.

Zink BJ, Stern SA, Wang X, Chudnofsky CC. Effects of ethanol in an experimental model of combined traumatic brain injury and hemorrhagic shock. Acad Emerg Med 1998;5(1):9–17.